

First-Principles Study of the Diffusion of Hydrogen in ZnO

M. G. Wardle, J. P. Goss, and P. R. Briddon

School of Natural Sciences, University of Newcastle upon Tyne, Newcastle upon Tyne, NE1 7RU, United Kingdom

(Received 4 November 2005; published 26 May 2006)

Zinc oxide, a wide-gap semiconductor, typically exhibits *n*-type conductivity even when nominally undoped. The nature of the donor is contentious, but hydrogen is a prime candidate. We present *ab initio* calculations of the migration barrier for H, yielding a barrier of less than ~ 0.5 eV. This indicates isolated hydrogen is mobile at low temperature and that thermally stable H-related donors must logically be trapped at other defects. We argue this is also true for other oxides where H is a shallow donor.

DOI: 10.1103/PhysRevLett.96.205504

PACS numbers: 61.72.Vv, 61.72.Bb, 71.15.Nc, 71.55.Gs

Zinc oxide has become a prominent material for wide-gap semiconductor, optoelectronic, and, via doping with transition metals, spintronics applications.

Production of ZnO devices has been hindered by difficulties in fabricating *p*-type material due to nominally undoped material typically exhibiting strong *n*-type conductivity. Interstitial hydrogen (H_i), known to be a shallow donor [1–3], is a possible source of this conductivity. Indeed, hydrogen acting as a dopant is potentially a widespread phenomenon in compound semiconductors including many oxides [4–6]. However, in order for such doping to be technologically relevant, the thermal stability of the H-donor must be sufficient to prevent degradation during operation of devices at and above room temperature.

Theoretically, in ZnO isolated H_i forms a strong bond with oxygen, lying either in a bond-centered or an anti-bonding location. Both forms result in a Zn neighbor displaced from the host site, away from the O-H group [1,7]. Because ZnO adopts the wurtzite (hexagonal) crystal form, there are distinct sites aligned along the *c* axis of the material (\parallel) and in the basal plane (\perp) as shown in Fig. 1. It has been shown theoretically [7–9] that BC_{\parallel} is lowest in energy, with just ~ 0.2 eV covering the four structures in Figs. 1(b)–1(e).

The role of *isolated* H_i as a thermally stable dopant may be questioned as deuterium is reported to diffuse readily, with an activation energy of just 170 meV [10]. However, *n*-type conductivity persists in material annealed to 600 °C [10]. ZnO intentionally doped with hydrogen displays an increase both in free carrier concentration and infrared (ir) band intensity [9,11]. The increase in carrier concentration is subsequently reduced by 80% by a 150 °C anneal for 30 min, along with the loss of the ir bands [12]. ir-band intensities are also lowered in samples stored at room temperature over time scales of weeks [13]. However, subsequent high-temperature annealing restores these ir bands, perhaps indicating that the room-temperature anneal is leading to formation of more stable, perhaps electrically inactive defects.

In addition to ir, bound-exciton luminescence also has to be attributed to thermally stable hydrogen [14–16]. For

example, the I_4 line is reduced above 600 °C [14]. Photoconductivity shows that there are many distinct H-related donors [16], consistent with H being located close to a secondary defect.

Lattice vacancies and impurities may trap hydrogen, reducing the H_i -donor concentration. Impurity-hydrogen complexes are quite stable with the activation barrier for the loss of hydrogen in Cu-doped material being 0.91 eV [17]. Indeed, ir bands associated with Cu-H (Cu-I), Li-H (H-I*), and V_{Zn} - H_2 (H-II) are removed by annealing at relatively high temperatures [9,18], further suggesting rather stable defects.

In this Letter we show, based on *ab initio* density-functional calculations, that hydrogen is likely to be a highly mobile species in the absence of trapping sites. Several diffusion paths are investigated, with the classical barrier for each determined.

We employ density-functional techniques within the local density approximation as embodied in the AIMPRO (*Ab Initio* Modeling PROgram [19,20]) code, with periodic boundary conditions. We remove the core electrons by the use of pseudopotentials [21], with the valence wave functions described using a basis of sets of independent *s*-, *p*-, and *d*-Gaussian orbitals with four different exponents sited at each atom site. We have performed calculations both explicitly including the 3*d* electrons of the Zn atoms, or more typically by using a nonlinear core-correction. We

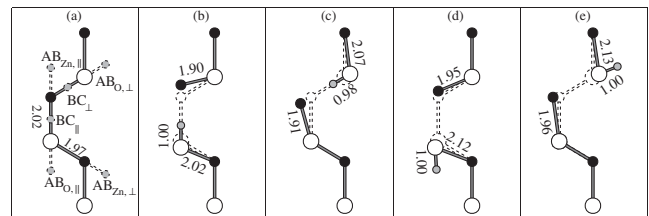


FIG. 1. (a) Schematic showing sites for H in ZnO. (b), (c), (d), (e) show structures subsequent to relaxation with the ideal sites indicated by dashes. Black, white, and gray circles represent Zn, O, and H atoms, respectively. The vertical and horizontal axes are $[0001]$ and $[2\bar{1}\bar{1}0]$. All bond lengths are given in Å.

find no appreciable differences either in structure, defect levels, or diffusion barriers. Commonly it is held that generalized-gradient approximation (GGA) calculations treat bond-breaking reactions more accurately than the local density approximation. Therefore we have also performed GGA [22] calculations, using a different set of pseudopotentials [23] where we include the Zn 3*d* electrons in the valence.

Typically, a regular mesh of 2^3 **k** points are used to sample the band structure [24], and the charge density is Fourier transformed using plane waves with an energy cutoff of 300 Ry. The Zn and O basis sets reproduce the lattice constants of wurtzite ZnO (*w* ZnO) to within 0.4%. The calculated band gap of 1.3 eV (which greatly underestimates the experimental direct band gap of around 3.4 eV) is within the range previously reported [1,25–27].

Unless otherwise stated, results relate to a 96-atom orthorhombic supercell, with vectors $[3\bar{3}00]a$, $[22\bar{4}0]a$, and $[0002]c$ relative to the primitive *w* ZnO lattice vectors.

In most instances we use the well-established climbing nudged-elastic-band (C-NEB) technique [28] to determine the saddle-point structures and energies. In addition, in a number of cases estimates of barriers were obtained by relaxing geometries subject to the constraint that the H atom lies midway between two oxygen atoms.

The diffusion paths investigated are those for H_i^+ originating at what we find [7] to be the lowest energy structure ($H_{BC_{\parallel}}$), moving to an equivalent adjacent site. We have also calculated the migration barrier for H_i^0 , and find it to be within 30 meV of the positive case. This is entirely consistent with the shallow nature of the donor level, which implies a diffuse donor wave function and is therefore not expected to greatly change the strengths of bonds in the vicinity of the migrating impurity.

Schematic representations of the steps in the diffusion paths are shown in Fig. 2. We highlight four overall routes: the first represents the diffusion of hydrogen in the basal plane ($1 \rightarrow 2 \rightarrow 1$, denoted as path A), and three paths propagate parallel to the *c* axis ($1 \rightarrow 3 \rightarrow 4 \rightarrow 6$, path B; $1 \rightarrow 3 \rightarrow 4 \rightarrow 5 \rightarrow 1$, path C; and $7 \rightarrow 6$, path D).

All of the diffusion paths involve reorientation steps in which the hydrogen remains bonded to the same oxygen atom. Of these steps, 1, 3, and 4 in Fig. 2 have relatively low barriers, 0.21, 0.24, and 0.29 eV, respectively, relative to the ground-state structure ($H_{BC_{\parallel}}$). Reorientation in a clockwise direction in Fig. 2 (path 7), remaining in the (1000) plane, not passing through a BC_{\perp} structure, is 0.1 eV higher than the path $1 \rightarrow 3 \rightarrow 4$. The reorientation of H about a single oxygen atom is therefore energetically very favorable and is likely to proceed at relatively low temperatures.

We shall first discuss the diffusion of H within a basal plane, path A. The energetically favored path involves two stages: first the low-energy reorientation of an O-H bond from BC_{\parallel} to $AB_{O_{\perp}}$, followed by the breaking of this O-H

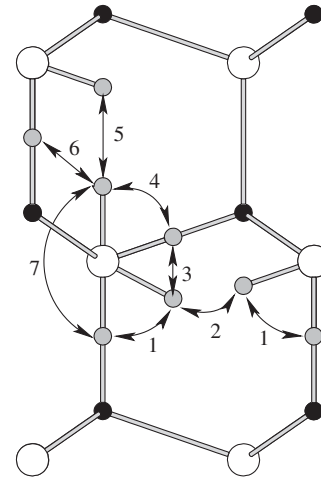


FIG. 2. Schematic representation of the possible diffusion paths of H in ZnO. Steps 1–7 represent steps between stable structures. Atom colors and axes are as in Fig. 1.

bond and the formation of another. It is instructive to also observe the strengthening and weakening of the O-Zn interactions during this process. Initially, there is a single “broken” O-Zn bond, i.e., that containing the H atom. As the O-H bond rotates to form $AB_{O_{\perp}}$, this broken O-Zn bond reforms, but a second Zn-O bond, approximately perpendicular to the *c* axis, is weakened [Fig. 1(e)]. The barrier to reorientation is therefore dominated by the ionic O-Zn bonds, so that the low activation energy can be understood as arising from the relatively weak energy dependence of ionic bond length and angle deformation.

The second part of the diffusion relates to changes in O-H bonds, which are more covalent in nature. As shown in Fig. 3(a), the making and breaking of O-H bonds costs more energy than the reorientation, and thus the “hop” between neighboring oxygen atoms represents the rate-limiting step in the diffusion of H in ZnO. Diffusion in the basal plane is calculated to have a barrier of ~ 0.4 eV.

The saddle-point structure places the H atom equidistant from the two O atoms between which it is hopping, as shown schematically in Fig. 4(a). The simplicity of the saddle-point structure for in-plane diffusion allows us to gain an accurate estimate of the error bars on the barrier heights arising from computational parameters: (i) Explicitly including the 3*d* electrons of zinc as valence electrons in the pseudopotential yields a barrier just 60 meV higher than when using the nonlinear core-correction; (ii) Increasing the Brillouin-zone sampling from $2 \times 2 \times 2$ to $4 \times 4 \times 4$ changes the activation by just 6 meV; (iii) Calculations performed in smaller, 36-atom supercells [3×3 repeats of the four-atom primitive unit-cell in the (0001) plane] yields a barrier of ~ 0.6 eV; (iv) For a larger supercell containing 144 host-atoms (increasing the supercell in the *c* direction by 50% relative to the 96-atom supercell) the activation energy increases to around 0.5 eV; (v) GGA calculations in 96-atom cells yield 0.6 eV.

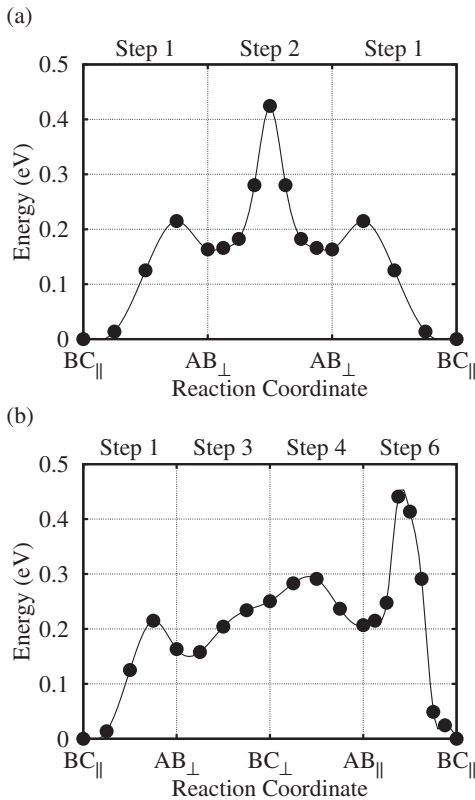


FIG. 3. Migration barrier calculated using C-NEB for the diffusion of H_i^+ in w ZnO (a) along the basal-plane diffusion path A (Fig. 2), and (b) in the axial direction via path B. The circles are calculated points and the curves a guide to the eye. Steps are as labeled in Fig. 2.

Since the various calculations yield very similar barriers, we conclude that diffusion of H_i^0 and H_i^+ in the basal plane may proceed with an activation energy of around 0.5 eV, with an error bar of around 0.1 eV.

Since the lattice is anisotropic, in principle there may be a significantly different barrier to diffusion perpendicular

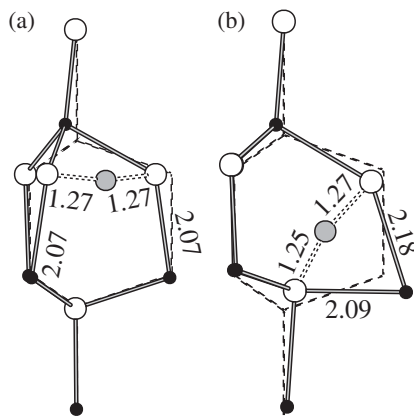


FIG. 4. Saddle-point structures for the rate-limiting steps in (a) the basal-plane diffusion and (b) the axial diffusion. Colors and axes are as in Fig. 1.

to the basal planes. For the three paths (B, C, and D) outlined above involved in the diffusion of hydrogen along the c axis, there are a number of reorientation steps, in analogy with the in-plane diffusion. In these reorientation processes, the hydrogen remains bonded to a single oxygen, with one or more O-Zn bonds being stretched or broken (see Fig. 1). Again in line with the basal diffusion, the rate-limiting step is that in which the hydrogen is transferred from one oxygen to another, i.e., the breaking of the $AB_{O_{\parallel}}$ bond and making of the $AB_{O_{\perp}}$ or BC_{\parallel} bonds (step 5 or 6 in Fig. 2, respectively).

The diffusion profile was calculated via C-NEB for each of these paths, with that obtained for path B shown in Fig. 3(b). Since all three diffusion paths are limited by the hop rather than reorientation, they only differ in the details of the reorientation barriers and therefore have the same barrier height of around 0.4 eV in the 96-atom supercell. Therefore we find that the classical barrier to diffusion in the c -axis direction is not significantly different from that within the basal planes, indicating that hydrogen should diffuse throughout bulk w ZnO, regardless of crystallographic direction.

As with the in-plane diffusion, the saddle point can be characterized as a bridging site between two O atoms, with the structure shown schematically in Fig. 4(b).

It is worth noting that the barriers presented above do not take into account any tunneling and vibrational effects in the motion of H. The distance between H sites in the hop between neighboring O sites is just 1.08 Å, which may be considered as the order of magnitude for the potential barrier width. We have modeled the stretch mode of $AB_{O_{\perp}}$ by calculating the vibrational potential along the O-H bond direction, and solving the one-dimensional Schrödinger equation of the oscillator [29]. The *ground-state* anharmonic wave function calculated in this fashion extends to around 0.5 Å beyond the equilibrium location, with higher oscillator states naturally extending even further. The vibrational modes may be used to estimate the zero-point energy, from which a reduction to the activation energy of the order of 0.1 eV has been determined. In addition, the energy associated with the stretch mode at around 0.4 eV is close to the barrier height, so that its absorption may stimulate migration.

One must therefore consider the 0.5 ± 0.1 eV classical estimate of the barrier an overestimate when vibrational motion and tunneling effects are taken into account, supporting the rather low experimental barrier for deuterium diffusion [10]. The limitations of the barrier height estimate prevent us from determining a precise temperature at which H_i becomes mobile. However, a simple Arrhenius relation suggests mobility at or below 200 K, certainly well below room temperature.

In summary, we have used first-principles methods to obtain estimates of the activation energy for the diffusion of H in w ZnO. The barrier is only very weakly dependent

on charge state, consistent with the shallow nature of the donor level, and shows no significant variation with diffusion direction. The values of 0.4–0.5 eV determined using the 96-atom supercell are smaller than those obtained experimentally, suggesting that trap-limited diffusion is dominant even in undoped *w* ZnO materials. The activation barrier of ~ 1 eV for the loss of the 3326 cm^{-1} ir band [13,30] is considerably higher than the calculated barrier for diffusion of H_i . However, Jokela *et al.* suggest that the loss of the ir band can be explained by the formation of hydrogen molecules, which are electrically inactive and difficult to detect spectroscopically. If their model is correct, then our calculations suggest that the 1 eV would correspond to the formation of the molecules rather than the diffusion of H_i , but we note that binding energies of hydrogen to common impurities such as lithium and first-row transition metals are also often around this value [7,31–33].

The mobility of H_i in ZnO has major implications for the interpretation of experimental observations. First, the H-related infrared absorption and bound-exciton luminescence seen to be stable to relatively high temperatures (such as seen for H-I*, Cu-I and H-II bands stable to above 350°C , and the I_4 luminescence stable above 600°C) are most likely associated with H *trapped* at a secondary defect.

Secondly, the thermally stable *n*-type doping, if related to hydrogen, must relate to H trapped at an electrically inactive trapping site. Indeed, the fact that there are several variants of the H-related donor [16,18] is consistent with this interpretation, and we have shown previously that $\text{Cu}_{\text{Zn}}\text{-H}_2$ complexes are an example of trapped hydrogen forming shallow donors [34].

Finally, although the results presented here relate to zinc oxide, this material is one of several in which hydrogen is predicted to be a shallow donor. Others include [4–6] CdO, SnO_2 , TiO_2 , HfO_2 , ZrO_2 , and SrTiO_3 (many others having been suggested). At least for the cases mentioned, the interoxygen distances are comparable or smaller than in ZnO. In particular, the dioxides have O-O separations of around 80% of that in *w* ZnO. Since the predicted migration path for H in ZnO is dominated by hops between O sites, the barriers will be controlled by the O-H bond strength and the dilation of this bond in the saddle-point structure. It therefore seems entirely plausible that hydrogen will also migrate rapidly in these other important cases. Calculations are underway to test this hypothesis.

[1] C.G. Van de Walle, Phys. Rev. Lett. **85**, 1012 (2000).
 [2] S.F.J. Cox *et al.*, Phys. Rev. Lett. **86**, 2601 (2001).
 [3] D.M. Hofmann *et al.*, Phys. Rev. Lett. **88**, 045504 (2002).

[4] S.F.J. Cox, J. Phys. Condens. Matter **15**, R1727 (2003).
 [5] P.W. Peacock and J. Robertson, Appl. Phys. Lett. **83**, 2025 (2003).
 [6] Ç. Kiliç and A. Zunger, Appl. Phys. Lett. **81**, 73 (2002).
 [7] M.G. Wardle, J.P. Goss, and P.R. Briddon, Phys. Rev. B **72**, 155108 (2005).
 [8] S. Limpijumngong and S.B. Zhang, Appl. Phys. Lett. **86**, 151910 (2005).
 [9] E.V. Lavrov *et al.*, Phys. Rev. B **66**, 165205 (2002).
 [10] K. Ip *et al.*, Appl. Phys. Lett. **82**, 385 (2003).
 [11] M.D. McCluskey *et al.*, Appl. Phys. Lett. **81**, 3807 (2002).
 [12] G.A. Shi *et al.*, Phys. Rev. B **72**, 195211 (2005).
 [13] S.J. Jokela, M.D. McCluskey, and K.G. Lynn, Physica (Amsterdam) **340–342B**, 221 (2003).
 [14] B.K. Meyer *et al.*, Phys. Status Solidi B **241**, 231 (2004).
 [15] A.V. Rodina *et al.*, Phys. Rev. B **69**, 125206 (2004).
 [16] E.V. Lavrov, F. Börrnert, and J. Weber, Phys. Rev. B **72**, 085212 (2005).
 [17] F.G. Gartner and E. Mollwo, Phys. Status Solidi B **89**, 381 (1978).
 [18] E.V. Lavrov, F. Börrnert, and J. Weber, Phys. Rev. B **71**, 035205 (2005).
 [19] R. Jones and P.R. Briddon, in *The ab initio Cluster Method and the Dynamics of Defects in Semiconductors, Semiconductors and Semimetals* Vol. 51A (Academic Press, Boston, 1998), Chap. 6.
 [20] J.P. Goss, M.J. Shaw, and P.R. Briddon, Top. Appl. Phys. (to be published).
 [21] N. Troullier and J.L. Martins, Phys. Rev. B **43**, 1993 (1991).
 [22] J.P. Perdew, K. Burke, and M. Ernzerhof, Phys. Rev. Lett. **77**, 3865 (1996).
 [23] C. Hartwigsen, S. Goedecker, and J. Hutter, Phys. Rev. B **58**, 3641 (1998).
 [24] H.J. Monkhorst and J.D. Pack, Phys. Rev. B **13**, 5188 (1976).
 [25] A.F. Kohan, G. Ceder, D. Morgan, and C.G. Van de Walle, Phys. Rev. B **61**, 15019 (2000).
 [26] F. Oba, S.R. Nishitani, S. Isotani, and H. Adachi, J. Appl. Phys. **90**, 824 (2001).
 [27] W.R.L. Lambrecht *et al.*, Phys. Rev. B **65**, 075207 (2002).
 [28] G. Henkelman, B.P. Uberuaga, and H. Jónsson, J. Chem. Phys. **113**, 9901 (2000); **113**, 9978 (2000).
 [29] R. Jones, J. Goss, C. Ewels, and S. Öberg, Phys. Rev. B **50**, 8378 (1994).
 [30] S.J. Jokela and M.D. McCluskey, Phys. Rev. B **72**, 113201 (2005).
 [31] E.-C. Lee and K.J. Chang, Phys. Rev. B **70**, 115210 (2004).
 [32] M.G. Wardle, J.P. Goss, and P.R. Briddon, Phys. Rev. B **71**, 155205 (2005).
 [33] C.H. Park and D.J. Chadi, Phys. Rev. Lett. **94**, 127204 (2005).
 [34] M.G. Wardle, J.P. Goss, and P.R. Briddon, Physica B (Amsterdam) **376**, 731 (2006).